J Nanostruct 11(2): 368-376, Spring 2021

RESEARCH PAPER

Synthesis and Morphological Investigation of Hydroxyapatite/ Zinc Oxide and Evaluation its Application in Removal of Organic Pollutants

Ratna Komala Dewi [1], Hamzah H. Kzar [2], Wanich Suksatan [3], Imam Taukhid [4], Hendrik Setia Budi [5], Ayad F. Alkaim [6], Surendar Aravindhan [7]

[1] *Department of Dermatology and Venereology, Bhakti Kartini Hospital, Margahayu, Indonesia*

[2] *Department of chemistry, College of Veterinary Medicine, Al-Qasim green university, Iraq*

[3] *Faculty of Nursing, HRH Princess Chulabhorn College of Medical Science, Chulabhorn Royal Academy, Thailand*

[4] *Ministry of Marine and Fisheries Affairs, Research Institute For Coastal Aquaculture And Fisheries Extention, Indonesia*

[5] *Department of Oral Biology, Faculty of Dental Medicine, Universitas Airlangga, Indonesia*

[5] *College of science for women, University of Babylon, Iraq*

[6] *Department of Pharmacology, Saveetha dental College and hospital, Saveetha institute of medical and technical sciences, Chennai, India*

ARTICLE INFO

Article History:
Received 18 October 2020
Accepted 05 March 2021
Published 01 April 2021

Keywords:
Azo dyes
Hydroxyapatite
Nanocomposites
Photocatalyst

ABSTRACT

Water contamination has negative effects on people's quality of life and the environment in recent decades as a result of increased agricultural and industrial activities. Using new advanced nanomaterials can be helpful for the removal of water contamination. In this study, novel hydroxyapatite/ zinc Oxide nanocomposites was prepared via a simple ci-precipitation route. Hydroxyapatite has been known as a biocompatible nanomaterial. Prepared samples were analyzed via X-ray diffraction (XRD), scanning electron microscopy (SEM), energy-dispersive X-ray spectroscopy (EDS), and Fourier-transform infrared spectroscopy (FTIR) analysis. It was found that hydroxyapatite/zinc Oxide nanocomposites can be provided as an attractive candidate for photocatalytic degradation of azo dyes. The prepared Hydroxyapatite/Zinc Oxide nanocomposites were utilized as a photocatalyst for degradation of methylene blue and acid blue 92. Results showed that prepared hydroxyapatite/zinc Oxide nanocomposites can be degraded 87% and 98% of rhodamine B and methylene blue under UV irradiation respectively. It was observed that hydroxyapatite improve the photocatalytic activity of zinc oxide.

How to cite this article
Komala Dewi R, Kzar H. H, Suksatan W, Taukhid I, Setia Budi H, Alkaim A. F, Aravindhan S. Synthesis and Morphological Investigation of Hydroxyapatite/Zinc Oxide and Evaluation its Application in Removal of Organic Pollutants. J Nanostruct, 2021; 11(2):368-376. DOI: 10.22052/JNS.2021.02.016

INTRODUCTION

Organic pollutants are becoming more prevalent in water sources around the world as the world's population grows and industrial and agricultural development continues [1, 2]. Biological treatment procedures could be used to remediate wastewater with high levels of biodegradable contaminants [3]. However, wastewater from a variety of

* *Corresponding Author Email: dorkoosh@tums.ac.ir*

industries, including textile, pharmaceutical, and agricultural, frequently contains harmful chemicals that are slow to degrade [4-6]. Despite the fact that there are many promising chemical treatment solutions, oxidizing agents employed in the water treatment process are having trouble dissolving and mineralizing the complicated structure of pollutants [7-9]. Photocatalysis is a viable method for addressing the water source pollution problems. The photocatalytic process begins when the catalyst is exposed to light and degraded pollutants via producing free radicals [10, 11]. The main problem in this technology is to design effective photocatalysts that meet several requirements, including photochemical and chemical stability, robust light absorption, and good charge separation [12-15]. While nanotechnology has yet to be studied in industrial water treatment processes, it offers a huge chance to ensure the efficacy of photocatalytic systems. The photocatalytic efficiency depends intensively on the applied catalyst, so nanostructures can be used in the photocatalysis process effectively [16-18]. Nanomaterials have size-dependent properties such as high surface area, high thermal stability, and excellent optical properties, which makes them an attractive option for photocatalytic processes [19, 20]. These characteristics are crucial because they can influence the material's use. According to this, the application of nanomaterials in the photocatalytic process have progressed rapidly in recent years. Various nanostructures have been prepared and applied for the improvement of separation photogenerated electrons and holes in the photocatalytic process [21-25]. Scientists have recently been inspired by zinc oxide (ZnO)-based nanocomposites' remarkable photocatalytic characteristic to create better ZnO-based nanocomposites with improved photo efficiency for pollutant degradation. In the synthesis and application of ZnO-based nanocomposites for the photocatalytic process, their biocompatibility is very important. So far, many ZnO-based nanocomposites have been made, but their toxic properties have made their application a major challenge [25-27]. To overcome this limitation, hydroxyapatite nanomaterials can be very helpful because of their superior biocompatibility. The photocatalytic performance of ZnO/hydroxyapatite nanocomposites depends heavily on the shape and size of ZnO and hydroxyapatite nanostructures [28, 29]. The shape and size of nanostructures are influenced by their synthesis procedures.

Karim Tanji et al. prepared zinc oxide/hydroxyapatite nanocomposites via the wet impregnation method. The followed method was applied for the synthesis of zinc oxide/hydroxyapatite nanocomposites: a naturally occurring phosphate ore rich in silica and calcium phosphate was sieved to separate the silica and phosphate phases. After that, a pure hydroxyapatite (HAP) was prepared using a chemical precipitation process, which was employed as a platform for ZnO immobilization which ws provided at two weight ratio (25%, and 50%). Then, the obtained nanocomposites was applied for photodegradation of caffeine and rhodamine B. Because hydroxyapatite increases the synergic phenomena of photocatalysis and adsorption, the conversion of both molecules grew faster and higher as a result of its presence. Results showed that after 25 and 60 min, rhodamine B and caffeine were completely photodegraded, respectively [30].

In another work, C. El Bekkali et al. prepared zinc oxide/hydroxyapatite nanocomposites via solvent-free route and investigated its photocatalytic efficiency against ofloxacin and ciprofloxacin antibiotics under UV irradiation. It is found that both antibiotics were degraded significantly. Depending on the antibiotic studied, the photocatalytic efficiency of the zinc oxide/hydroxyapatite nanocomposites under UV irradiation was equivalent to or better than that of the photocatalytic particles alone at high ZnO loadings [31].

In this work, the hydroxyapatite nanoparticles and zinc oxide/hydroxyapatite nanocomposites were prepared via a simple and fast chemical precipitation route. The shape, size, crystallinity, and optical properties of prepared nanocomposites were characterized via SEM, XRD, and UV-Vis analysis. The prepared nanocomposite was applied for photodegradation of methyl orange and rhodamine B under UV light.

MATERIALS AND METHODS

Chemical and reagents

Calcium nitrate ($Ca(NO_3)_2$), ammonium dihydrogen phosphate ($(NH_4)(H_2PO_4)$), polyvinylpyrrolidone (PVP), sodium hydroxide (NaOH), Zinc nitrate hexahydrate ($Zn(NO_3)_2{\cdot}6H_2O$), and ethanol were prepared from Merck Co.

and applied at analytical grade without further purification.

Field emission scanning electron microscopy (FESEM) (XL30, Philips microscope) was applied for the characterization of the shape and size of products. Fourier transform infrared (FTIR) spectra of the samples was provided via Magna-IR, spectrometer 550 Nicolet in KBr pellets. X-ray diffraction patterns were obtained by an X-ray diffractometer using Ni-filtered CuKα radiation, Philips. The optical properties of samples were investigated via UV-Vis spectrophotometer (UV-shimadzu).

Synthesis of hydroxyapatite

Calcium nitrate and ammonium dihydrogen phosphate was dissolved in deionized water according to the molar ratio 1.67:1 (Ca:P). Then, the pre-prepared PVP solution was added to the solution. After 20 min, the 0.01M NaOH was added to as-prepared Ca, and P containing solution dropwise under vigorous stirring. The

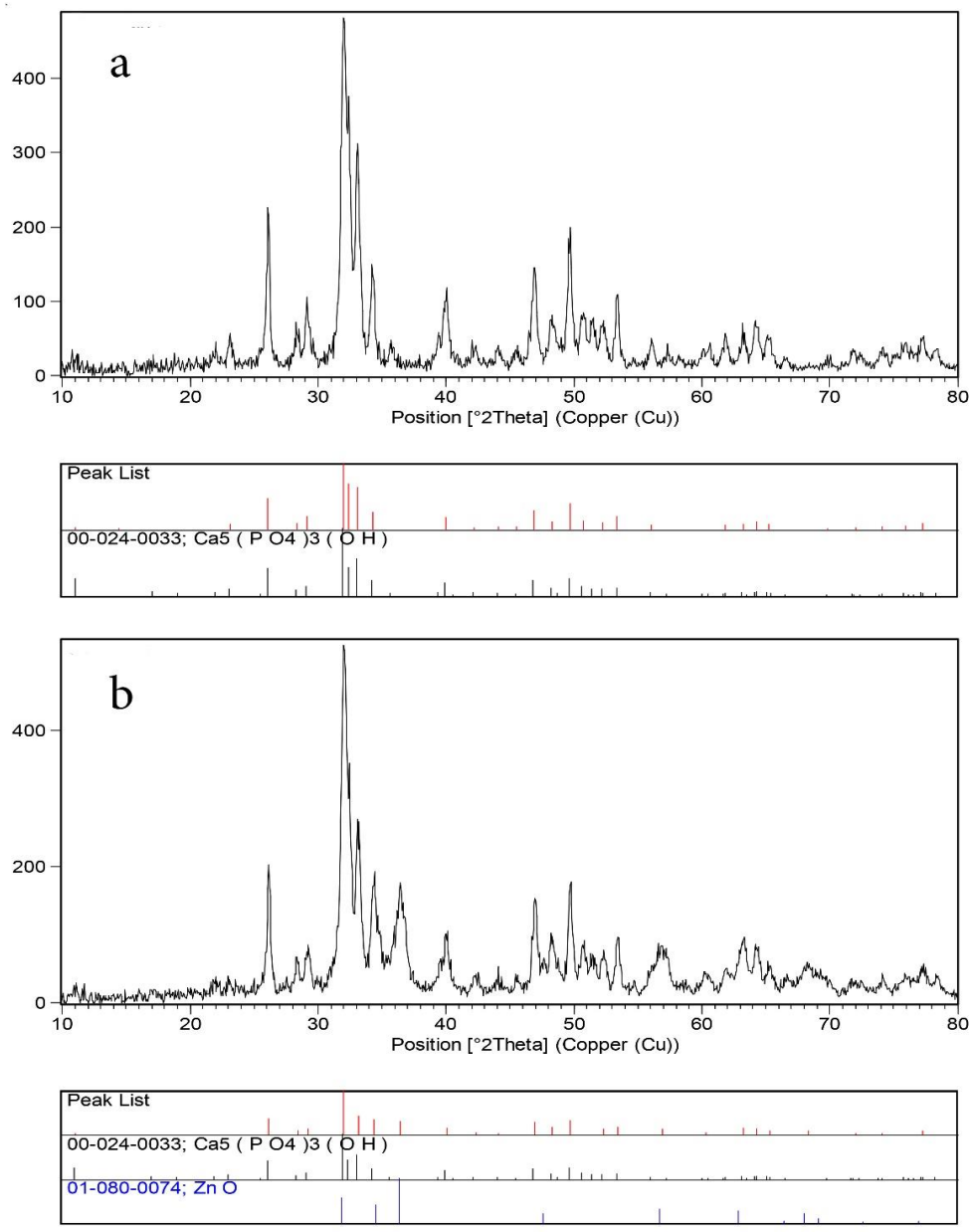

Fig. 1. XRD pattern of a) hydroxyapatite nanoparticles and b) zinc oxide/hydroxyapatite nanocomposites

pH of the solution was checked regularly. The addition of NaOH continued until reaching the pH of 10. The as-obtained mixture underwent 10 h of stirring. The collected white solid was washed with deionized water and ethanol. The white precipitate was dried at 60 ˚C for 20 h. The final product was obtained with sample calcination at 700 ˚C for 2 h.

Synthesis of zinc oxide/hydroxyapatite nanocomposites

The as-prepared hydroxyapatite nanomaterials were dispersed in deionized water in the ultrasonic bath. The Zinc nitrate hexahydrate was added to the mixture and stirred for 15 min. After that the NaOH solution was added to precipitate zinc hydroxide. Then, the prepared solid was centrifuged and then dried at 60 ˚C for 24 h. Finally, the solid was calcined at 500 ˚C for 2 h.

Photocatalytic test

In a batch photoreactor, methylene blue and rhodamine B photocatalytic degradation were employed to investigate the photocatalytic activity of zinc oxide/hydroxyapatite nanocomposites. The UV lamp was placed seven centimeters away from the solution surface. The zinc oxide/hydroxyapatite nanocomposites (0.2 g) was added to the 20 ppm methylene blue and rhodamine B solution and physically agitated for 30 minutes in the dark to achieve adsorption equilibrium. A mechanical stirrer was used to mix the contents of the reactor under UV irradiation. Then, every 15 minutes, using 5 minutes of centrifugation at 12,000 rpm, zinc oxide/hydroxyapatite nanocomposites was isolated from the samples collected from the photodegraded solution. The UV-vis analysis was used to determine the methylene blue and rhodamine B concentration.

RESULTS AND DISCUSSION

Crystalline structure of prepared hydroxyapatite nanoparticles and zinc oxide/hydroxyapatite nanocomposites was investigated via XRD. As well as shown in Fig. 1a, the hexagonal phase of hydroxyapatite was forms (JCPDS No. 00-024-0033, space group: P63/m) with lattice parameter a = b= 9.4320 Å and c = 6.8810. The crystalline size was calculated via Scherrer equation:

$$D_c=K\lambda/\beta Cos\theta \quad (1)$$

where β is the width of the observed diffraction peak at its half maximum intensity (FWHM), K is the shape factor, which takes a value of about 0.9, and λ is the X-ray wavelength (CuKα radiation, equals to 0.154 nm). The crystalline size was measured 17 nm for hydroxyapatite nanoparticles. It should be noted that the position of the peak in XRD pattern confirmed the formation of pure hydroxyapatite without impurity. Fig. 1b shows the XRD pattern of zinc oxide/hydroxyapatite nanocomposites. The results showed that the hexagonal phase of zinc oxide (ZnO) with JCPDS No. 01-080-0074, space group: P63mc was formed with hydroxyapatite (JCPDS No. 00-024-0033). Because of the zinc

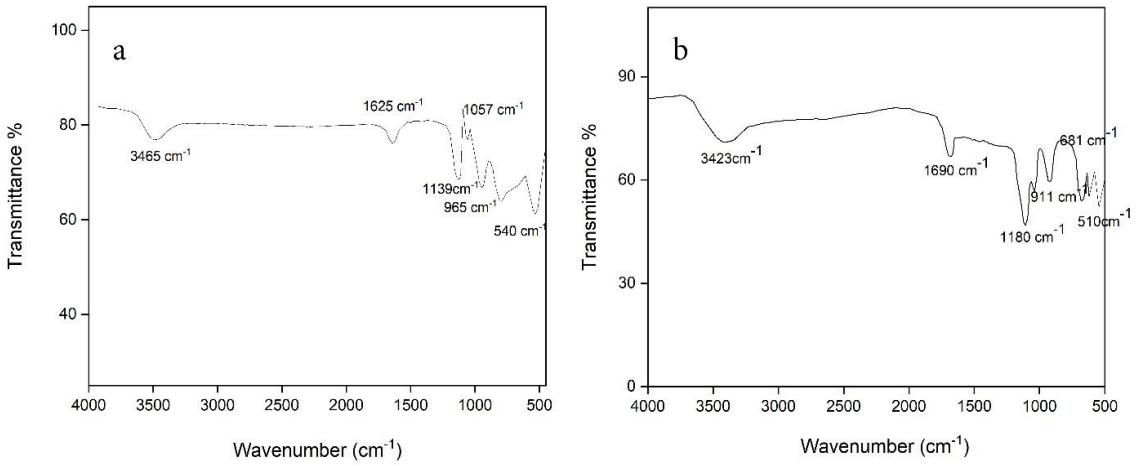

Fig. 2. FTIR spectrum of a) hydroxyapatite nanoparticles and b) zinc oxide/hydroxyapatite nanocomposites

oxide/hydroxyapatite nanocomposites synthesis, it was predictable that the phase structure of hydroxyapatite nanoparticles would not change. XRD analysis confirmed that the zinc oxide/ hydroxyapatite nanocomposites were successfully synthesized without impurity.

Fig. 2 shows FTIR spectrum of prepared hydroxyapatite nanoparticles and zinc oxide/ hydroxyapatite nanocomposites. The broad peaks at 3200-3500 cm^{-1} was attributed to the O-H bond. The mild peaks at near 540, 774, 900-970, 1000-1060, and 1100-1200 cm^{-1} were related to the PO_4^{3-}. The peak at 1600-1700 cm^{-1} was assigned to H-O-H absorption peak. The main difference between the FTIR spectrum of hydroxyapatite and zinc oxide/hydroxyapatite is the appearance of a peak at 5100 cm^{-1} which is related to the Zn-O bond. The intensity of O-H absorption peak in FTIR spectrum of zinc oxide/hydroxyapatite is lower than hydroxyapatite.

Fig. 3a shows SEM image of prepared hydroxyapatite nanoparticles. SEM images confirmed the formation of the regular shape and size of hydroxyapatite in 70 nm diameter. Fig. 3b shows the SEM images of prepared zinc oxide/hydroxyapatite nanocomposites. The SEM images display the formation of hydroxyapatite nanoparticles beside zinc oxide nanoparticles. The

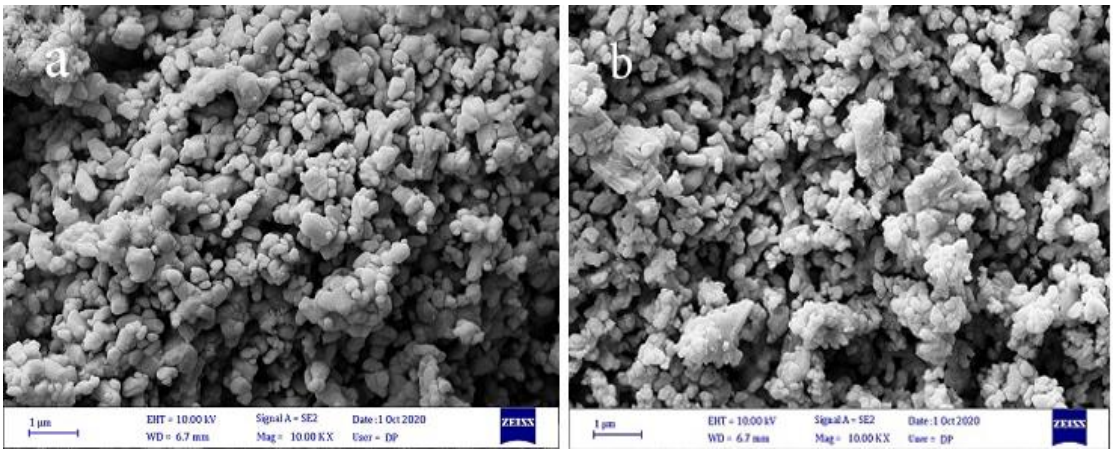

Fig. 3. SEM image of a) hydroxyapatite nanoparticles and b) zinc oxide/hydroxyapatite nanocomposites

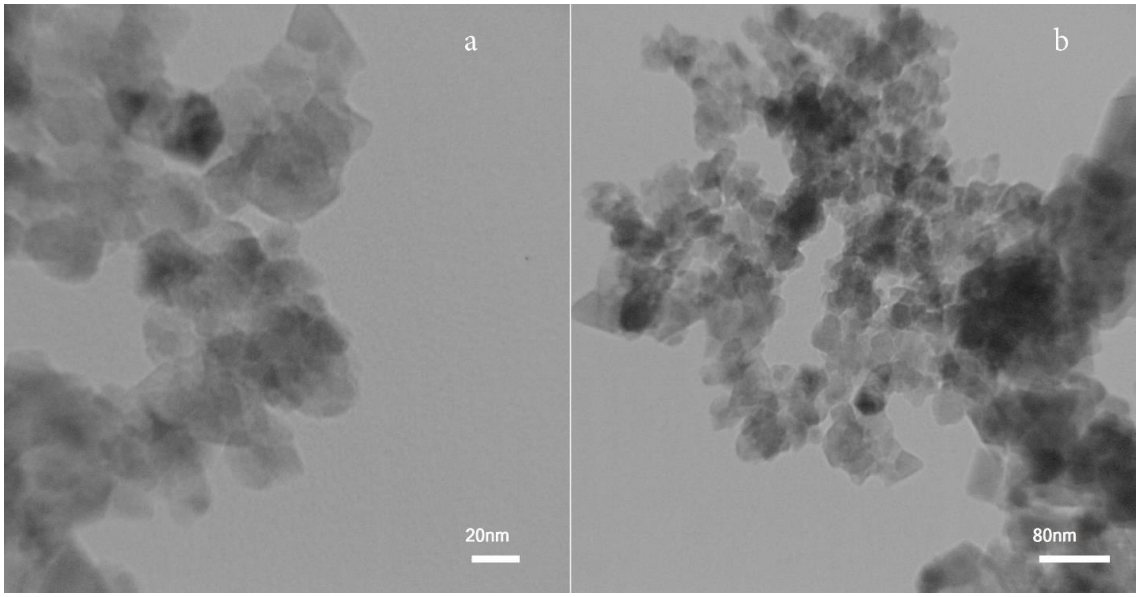

Fig. 4. TEM image of zinc oxide/hydroxyapatite at two magnifications

morphology of particles is spherical. TEM images were applied for further investigation of zinc oxide/ hydroxyapatite nanocomposites morphology. The obtained results from TEM images confirmed the formation of hydroxyapatite nanoparticles beside ZnO nanoparticles. It is also confirmed the homogenous shape and size of particles in prepared nanocomposites (Fig. 4). Optical properties are vital for photocatalytic application. Therefore, the UV-Vis analysis was applied for the investigation optical properties. As well as shown in Fig. 5a, the broad absorption peak was observed at 366 nm which is similar to the previous reports about ZnO-based nanocomposites [32, 33]. The optical energy band gap of nanocomposite was calculated via Tauc relation:

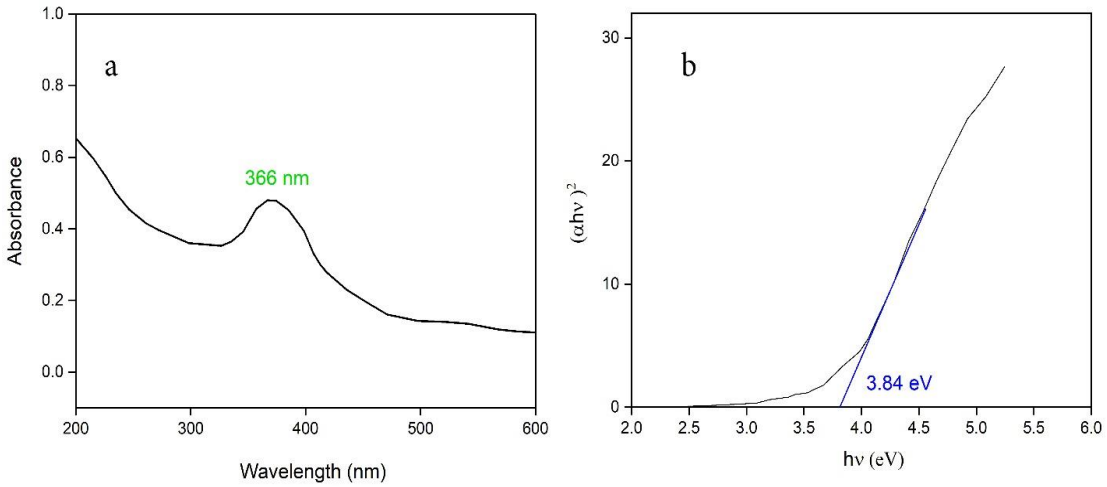

Fig. 5. a) UV-Vis absorption spectrum b) calculated band gap of prepared zinc oxide/hydroxyapatite

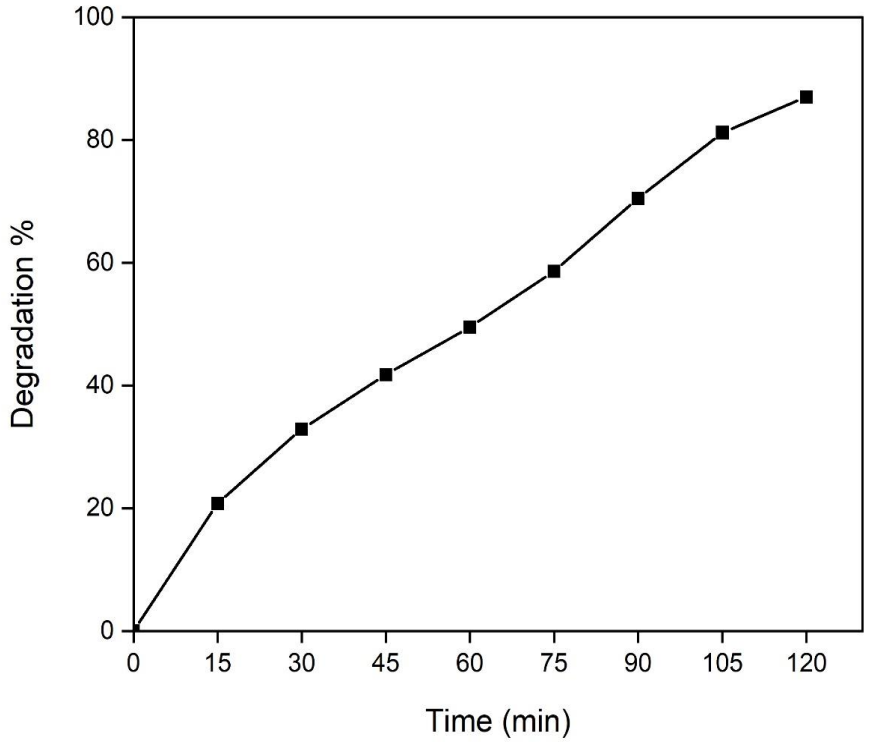

Fig. 6. Photocatalytic activity of prepared zinc oxide/hydroxyapatite against rhodamine B under UV irradiation

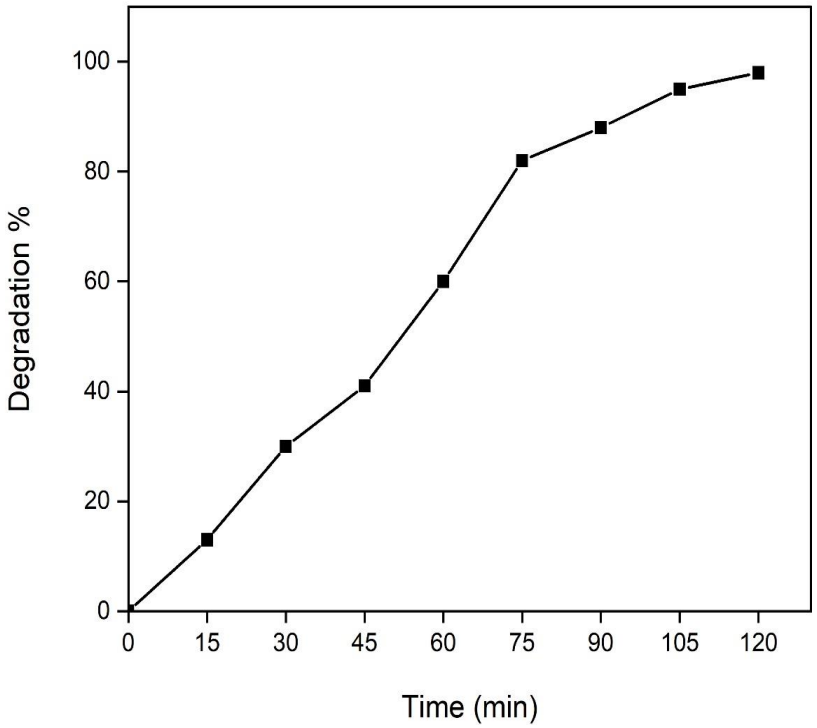

Fig. 7. Photocatalytic activity of prepared zinc oxide/hydroxyapatite against methylene blue under UV irradiation

$$(\alpha h\nu)^n = B(h\nu - E_g) \quad (2)$$

Where hν is the photo energy, α is the absorption coefficient, B is a constant relative to the material and n is either 2 for a direct transition or 1/2 for an indirect transition. The band gap was calculated 3.84 eV for prepared zinc oxide/ hydroxyapatite nanocomposites, as well as shown in Fig. 5b.

The water contaminant by dyes from different industries is raising a lot of concern in recent years. Despite their well-known toxicity to humans, azo dyes make up over half of the used dye population. In this study, prepared zinc oxide/hydroxyapatite nanocomposites was applied for photocatalytic degradation of methylene blue and rhodamine B as water pollutants. The photocatalytic efficiency was calculated via equation (3):

$$\text{Color Removal (\%)} = (C_0\text{-}C_t/\ C_0) \times 100 \quad (3)$$

Where C_0 (mgL^{-1}) is the initial concentration of methylene blue and rhodamine B in solution, and Ct (mgL^{-1}) is the concentration of methylene blue and rhodamine B at different irradiation times. Fig. 6 displays the photocatalytic activity of zinc oxide/hydroxyapatite nanocomposites against rhodamine b. It is clear that 87% of rhodamine B was degraded after 120 minutes under ultraviolet irradiation. The photocatalytic activity was increased 98% against methylene blue (Fig. 7). With more focus on details, it is clear that in the early times, the rate of degradation of methylene blue is higher than that of rhodamine B. The sufficient optical band gap leads to excellent photocatalytic activity of zinc oxide/hydroxyapatite nanocomposites. Optical features of zinc oxide/ hydroxyapatite nanocomposites cause charge transfer from zinc oxide to hydroxyapatite and stop charge recombination in zinc oxide. This led to the formation of hydroxyl radicals on the surface of nanocomposites and accelerates the photodegradation process.

CONCLUSION

In conclusion, hydroxyapatite nanoparticles and zinc oxide/hydroxyapatite nanocomposites were prepared via a facile and fast chemical precipitation route. The crystalline features of products were investigated via XRD analysis that confirmed the formation of hexagonal phase of

zinc oxide and hydroxyapatite. Morphological characteristics of samples were analyzed via SEM and TEM analysis. It was confirmed the regular spherical morphology of hydroxyapatite and zinc oxide/hydroxyapatite nanocomposites were formed. The band gap of prepared zinc oxide/hydroxyapatite nanocomposites was measure 3.84 eV through UV-Vis analysis which was excellent for the photocatalytic process under UV irradiation. Results showed that prepared zinc oxide/hydroxyapatite nanocomposites degraded 87% and 98% of rhodamine B and methylene blue after 120 minutes under UV irradiation. The presence of hydroxyapatite makes the zinc oxide/hydroxyapatite nanocomposites biocompatible.

CONFLICT OF INTEREST

The authors declare that there is no conflict of interests regarding the publication of this manuscript.

REFERENCES

1. Prakash J. Potential application of endophytes in bioremediation of heavy metals and organic pollutants and growth promotion: mechanism, challenges, and future prospects. Bioremediation for Environmental Sustainability: Elsevier; 2021. p. 91-121.
2. Santana-Viera S, Montesdeoca-Esponda S, Guedes-Alonso R, Sosa-Ferrera Z, Santana-Rodríguez JJ. Organic pollutants adsorbed on microplastics: Analytical methodologies and occurrence in oceans. Trends in Environmental Analytical Chemistry. 2021;29:e00114.
3. Boudh S, Singh JS, Chaturvedi P. Microbial resources mediated bioremediation of persistent organic pollutants. New and Future Developments in Microbial Biotechnology and Bioengineering: Elsevier; 2019. p. 283-94.
4. Mouele ESM, Tijani JO, Fatoba OO, Petrik LF. Degradation of organic pollutants and microorganisms from wastewater using different dielectric barrier discharge configurations—a critical review. Environmental Science and Pollution Research. 2015;22(23):18345-62.
5. Rasalingam S, Peng R, Koodali RT. Removal of Hazardous Pollutants from Wastewaters: Applications of TiO2-SiO2Mixed Oxide Materials. Journal of Nanomaterials. 2014;2014:1-42.
6. Sanderson H, Brown RS, Hania P, McAllister TA, Majury A, Liss SN. Antimicrobial Resistant Genes and Organisms as Environmental Contaminants of Emerging Concern: Addressing Global Public Health Risks. Management of Emerging Public Health Issues and Risks: Elsevier; 2019. p. 147-87.
7. Deng Y, Zhao R. Advanced Oxidation Processes (AOPs) in Wastewater Treatment. Current Pollution Reports. 2015;1(3):167-76.
8. Pal P. Chapter 6 - Industry-Specific Water Treatment: Case Studies. In: Pal P, editor. Industrial Water Treatment Process Technology: Butterworth-Heinemann; 2017. p. 243-511.
9. Oliveros E, Legrini O, Hohl M, Müller T, Braun AM. Industrial waste water treatment: large scale development of a light-enhanced Fenton reaction. Chemical Engineering and Processing: Process Intensification. 1997;36(5):397-405.
10. Lee S-Y, Park S-J. TiO2 photocatalyst for water treatment applications. Journal of Industrial and Engineering Chemistry. 2013;19(6):1761-9.
11. Houas A, Lachheb H, Ksibi M, Elaloui E, Guillard C, Herrmann J-M. Photocatalytic degradation pathway of methylene blue in water. Applied Catalysis B: Environmental. 2001;31(2):145-157.
12. Wu Q, Li D, Chen Z, Fu X. New synthesis of a porous Si/TiO2 photocatalyst: testing its efficiency and stability under visible light irradiation. Photochemical & Photobiological Sciences. 2006;5(7):653.
13. Wang Y-D, Lee T-W, Lo Y-C, Hong W-J, Chen C. Insights into photochemical stability of graphitic carbon nitride-based photocatalysts in water treatment. Carbon. 2021;175:223-32.
14. da Silva CG, Faria JLs. Photochemical and photocatalytic degradation of an azo dye in aqueous solution by UV irradiation. Journal of Photochemistry and Photobiology A: Chemistry. 2003;155(1-3):133-43.
15. Guo L, Jin S. Stable Covalent Organic Frameworks for Photochemical Applications. ChemPhotoChem. 2019;3(10):973-83.
16. Karimi H, Rajabi HR, Kavoshi L. Application of decorated magnetic nanophotocatalysts for efficient photodegradation of organic dye: A comparison study on photocatalytic activity of magnetic zinc sulfide and graphene quantum dots. Journal of Photochemistry and Photobiology A: Chemistry. 2020;397:112534.
17. Zarrabi M, Haghighi M, Alizadeh R. Enhanced sono-dispersion of Bi5O7I and Bi2ClHO3 oxides over ZnO used as nanophotocatalyst in solar-light-driven removal of methylene blue from water. Journal of Photochemistry and Photobiology A: Chemistry. 2019;370:105-16.
18. Sharma G, Gupta VK, Agarwal S, Bhogal S, Naushad M, Kumar A, et al. Fabrication and characterization of trimetallic nano-photocatalyst for remediation of ampicillin antibiotic. Journal of Molecular Liquids. 2018;260:342-50.
19. Sun CQ. Size dependence of nanostructures: Impact of bond order deficiency. Progress in Solid State Chemistry. 2007;35(1):1-159.
20. Miller RE, Shenoy VB. Size-dependent elastic properties of nanosized structural elements. Nanotechnology. 2000;11(3):139-47.
21. Abdolmohammad-Zadeh H, Zamani-Kalajahi M. In situ generation of H2O2 by a layered double hydroxide as a visible light nano-photocatalyst: Application to bisphenol A quantification. Microchemical Journal. 2020;158:105303.
22. Jiang Q, Han Z, Gao F, Cai C, Zhang J, Liu S, et al. Preparation of 3D porous microstructural nano-TiO2 photocatalyst with high efficiency based on Spilosoma niveus wings. Materials Chemistry and Physics. 2021;266:124519.
23. Fu Z, Zhao X, Zhang S, Fu Z. Preparation of nano-Zn2GeO4/rGO composite photocatalyst and its treatment of synthetic dye wastewater. Materials Chemistry and Physics. 2021;259:124004.
24. Bagheri S, Muhd Julkapli N. Nano-diamond based photocatalysis for solar hydrogen production. International Journal of Hydrogen Energy. 2020;45(56):31538-54.
25. Goktas S, Goktas A. A comparative study on recent progress in efficient ZnO based nanocomposite and heterojunc-

tion photocatalysts: A review. Journal of Alloys and Compounds. 2021;863:158734.
26. Sharma G, Kumar A, Sharma S, Naushad M, Dhiman P, Vo D-VN, et al. Fe3O4/ZnO/Si3N4 nanocomposite based photocatalyst for the degradation of dyes from aqueous solution. Materials Letters. 2020;278:128359.
27. Habibi-Yangjeh A, Pirhashemi M, Ghosh S. ZnO/ZnBi2O4 nanocomposites with p-n heterojunction as durable visible-light-activated photocatalysts for efficient removal of organic pollutants. Journal of Alloys and Compounds. 2020;826:154229.
28. Grenho L, Salgado CL, Fernandes MH, Monteiro FJ, Ferraz MP. Antibacterial activity and biocompatibility of three-dimensional nanostructured porous granules of hydroxyapatite and zinc oxide nanoparticles—anin vitroandin vivostudy. Nanotechnology. 2015;26(31):315101.
29. Heidari F, Bazargan-Lari R, Razavi M, Fahimipour F, Vashaee D, Tayebi L. Nano-hydroxyapatite and nano-hydroxyapatite/zinc oxide scaffold for bone tissue engineering application. International Journal of Applied Ceramic Technology. 2020;17(6):2752-61.
30. Tanji K, Navio JA, Chaqroune A, Naja J, Puga F, Hidalgo MC, et al. Fast photodegradation of rhodamine B and caffeine using ZnO-hydroxyapatite composites under UV-light illumination. Catalysis Today. 2020.
31. Bekkali CE, Bouyarmane H, Karbane ME, Masse S, Saoiabi A, Coradin T, et al. Zinc oxide-hydroxyapatite nanocomposite photocatalysts for the degradation of ciprofloxacin and ofloxacin antibiotics. Colloids and Surfaces A: Physicochemical and Engineering Aspects. 2018;539:364-70.
32. Talam S, Karumuri SR, Gunnam N. Synthesis, Characterization, and Spectroscopic Properties of ZnO Nanoparticles. ISRN Nanotechnology. 2012;2012:1-6.
33. Siva Vijayakumar T, Karthikeyeni S, Vasanth S, Ganesh A, Bupesh G, Ramesh R, et al. Synthesis of Silver-Doped Zinc Oxide Nanocomposite by Pulse Mode Ultrasonication and Its Characterization Studies. Journal of Nanoscience. 2013;2013:1-7.